Journal of Computer-Aided Molecular Design **18:** 13–22, 2004.

Molecular dynamics study of peptide segments of the BH3 domain of the proapoptotic proteins Bak, Bax, Bid and Hrk bound to the Bcl-x_L and Bcl-2 proteins

Marta Pinto[a,b], Juan J. Perez[b] & Jaime Rubio-Martinez[a,*]

[a]*Dept. de Química Física, Universitat de Barcelona (UB), Martí i Franqués 1, E-08028 Barcelona, Spain;* [b]*Dept. d'Enginyeria Química, Universitat Politècnica de Catalunya (UPC), ETS d'Enginyeria Industrial, Av. Diagonal 647, E-08028 Barcelona, Spain*

Received 18 December 2003; accepted in revised form 11 December 2003

Key words: apoptosis, Bcl-2 inhibition, drug design, molecular dynamics

Abstract

Overexpression of Bcl-2 and Bcl-x_L proteins, both inhibitors of apoptosis or *programmed cell death*, is related to the generation and development of several types of cancer as well as to an elevated resistance to chemotherapeutic treatments. Given that synthetic peptide fragments of the BH3 domain are capable to bind to both proteins and induce apoptosis in cell-free systems and HeLa cells, small molecule non-peptide mimics of these peptides can be considered as a new therapeutic strategy for the treatment of diseases associated to a deficient apoptosis or resistant to the treatments with chemotherapeutic drugs. This strategy is supported by experimental evidences about the death of transformed cells and sensibilization of tumoral cells by the inhibition of the antiapoptotic proteins Bcl-2 and Bcl-x_L. In the current work, these proteins complexed with X(16BH3), where X designates the proapoptotic proteins Bak, Bax, Bid and Hrk, have been modeled in order to establish a pharmacophoric hypothesis that must be present in any ligand capable of binding with the antiapoptotic proteins Bcl-2 and Bcl-x_L. The pharmacophore is also used to explain the structural features of a set of new small molecule inhibitors of these antiapoptotic proteins.

Introduction

Apoptosis or *programmed cell death* is a process by which cells commit suicide after completing their physiological function, or from a warning after a severe genetic damage has occurred. Moreover, this process can be inhibited through different signals [1–7]. However, it appears to be a common apoptotic mechanism preserved throughout evolution and regulated by the Bcl-2 family of proteins [8, 9]. The Bcl-2 gene was initially identified as an oncogene overexpressed in B-cell follicular lymphomas as a result of the chromosomic translocation t(14;18). Although Bcl-2 does not stimulate cellular proliferation, it extends the survival of the cell by inhibiting the programmed cell death in diverse tissues and in response to a great variety of stimuli [10, 11], through the regulation of a subgroup of cysteine proteases called caspases [12].

At least sixteen members of the Bcl-2 family of proteins have been sequenced in recent years, both in mammals and in viruses [13–15]. Some of them, such as Bcl-2, Bcl-x_L, Bcl-w or Mcl-1 block programmed cell death while others, such as Bad, Bak, Bax, Bid, Bim or Hrk, induce it. Although the mechanism of apoptosis regulation by Bcl-2 is not yet well understood, it has been shown that the relative amounts of pro- and antiapoptotic proteins determine the susceptibility of the cell to undergo apoptosis [16]. More specifically, it has been shown that the apoptotic activity of these proteins is related to their capability to form heterodimers [17]. Accordingly, it has been demonstrated that overexpression of Bcl-2 and Bcl-x_L proteins is related to the initiation and development of different

*To whom correspondence should be addressed. Phone: +34-93-4021222; Fax : +34-93-4021231; E-mail: j.rubio@qf.ub.es

types of cancer, as well as to an elevated resistance to chemotherapeutic treatments.

Proteins of the Bcl-2 family are characterized by exhibiting at least one of the four structural domains BH1–BH4 [8, 9]. Suppression of the BH3 domain of pro-apoptotic proteins prevents binding to antiapoptotic proteins like Bcl-2, Bcl-x_L or Ced-9 and results in a loss of their apoptotic activity [18]. Indeed, peptide fragments of the BH3 domain have been shown to induce apoptosis in cell-free systems and HeLa cells [19] by blocking the interaction between Ced-4, an analog to human Apaf-1, with Bcl-x_L [20, 21]. Accordingly, peptide fragments of the BH3 domain appear to compete with Apaf-1 for the binding groove formed by the BH1–BH3 domains of Bcl-x_L, considered to be necessary for its antiapoptotic activity [22].

These results suggest that peptide fragments of the BH3 domain of pro-apoptotic proteins can be considered as promising agents for the treatment of cancer. This strategy is supported by experimental evidence on the death of transformed cells and sensitization of tumoral cells by the inhibition of the antiapoptotic proteins Bcl-2 and Bcl-x_L [23, 24]. However, due to the difficulties associated with using peptides as therapeutic agents, small molecule non-peptide compounds, mimics of these peptides need to be considered for the development of a new therapeutic strategy for the treatment of diseases associated with deficient apoptosis or diseases resistant to the treatments with chemotherapeutic drugs. In this direction, five different groups have recently reported the discovery of small-molecule inhibitors of Bcl-2/ Bcl-x_L [25–29]. These compounds were found by virtual screening of different libraries, based on the assumption of binding to the cavity of Bcl-2, where the BH3 domains of the proapoptotic proteins do. The purpose of the present work is to characterize the structural requirements that these molecules need to exhibit for a good affinity to the Bcl-2 proteins, through a systematic studying of the structural features of different peptides with high affinity for Bcl-2.

The 3D structure of the heterodimer of Bcl-x_L and Bak BH3 domain peptide [30] evidences that the main feature of the recognition between the two proteins is the insertion of the BH3 domain of the latter, consisting of an amphipathic α-helix, in a hydrophobic groove formed by the BH1–BH3 domains of Bcl-x_L. Accordingly, in the present work, 16 different residue peptides corresponding to diverse BH3 domains of the proapoptotic proteins Bak, Bax, Bid and Hrk, shown to exhibit proapoptotic behavior, were docked into the hydrophobic groove of Bcl-x_L and Bcl-2. Moreover, molecular dynamics simulations of the complexes were conducted in order to investigate their stability along the dynamics process, and to properly characterize the most important structural features involved in the recognition process.

Methods

Molecular dynamics of the Bcl- x_L /X(16BH3) complexes

The sequences of the different hexadecapeptide fragments of the pro-apoptotic proteins Bak, Bax, Bid and Hrk studied in the present work (in general terms referred to as X(16BH3), where X is the name of the pro-apoptotic protein), were selected from a multiple sequence alignment of the BH3 domains shown in Figure 1. Starting structures for molecular dynamics studies of the BH3 fragments bound to Bcl-x_L, were generated using the NMR structure of the Bcl-x_L /Bak (16BH3) complex (entry 1BXL of the Protein Data Bank) [30] as template. For this purpose, the coordinates of the backbone atoms of Bcl-x_L and Bak hexadecapeptide fragment, together with those of the side chain atoms of matching residues in the sequence alignment, were taken from the experimental structure. Coordinates of the side chain atoms of non-matching residues were generated in an extended conformation using the EDIT module of the AMBER suite of programs [31].

Energy minimizations were carried out *in vacuo* using the parm94 force field [32] within the AMBER suite of programs [31], with a distance dependent dielectric constant of 4r to screen for electrostatic interactions. In a first step, only atoms of the side chains were allowed to move, while the rest of them were kept frozen. Next, side chains and backbone of the Bcl-x_L protein together with the side chains of the 16BH3 peptide were optimized. Finally, all the atoms of the system were allowed to relax. After energy minimization, complexes were solvated with a drop of TIP3 waters, located in such a way that all the atoms involved in the receptor-ligand interaction region were solvated. The cap included 980 water molecules and had a radius of 23 Å. Water molecules were subjected to a soft harmonic potential to restrain their movements and non-solvated atoms were restricted using the belly option. Non-bonded interactions were computed using a cutoff of 12 Å and a

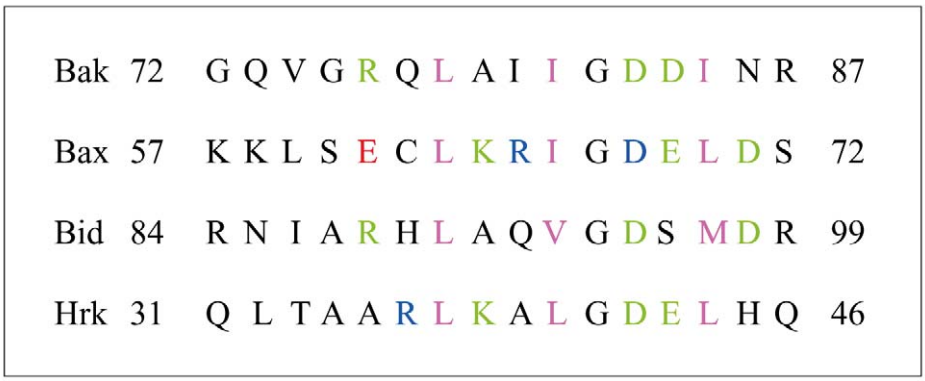

Figure 1. X (16BH3) sequences employed for the structural characterization of the complexes Bcl-2/X (16BH3) and Bcl-x_L/X (16BH3). In red, blue and green those amino acids that appear as important for interaction only with Bcl-x_L, only with Bcl-2 and with both, respectively. In fuchsia the hydrophobic residues considered as important for binding.

distance dependent dielectric constant of 1r was used for the electrostatic contribution. Energy minimization of the solvated complex was carried out in several steps. First, only the atoms of the side chains were optimized, keeping frozen the backbone atoms of both Bcl-x_L and 16BH3. The resulting structure was then subjected to a new minimization where all the atoms of Bcl-x_L protein and the 16BH3 peptide were allowed to vary. Finally, atoms of the complex structure and water molecules were completely relaxed. The structures were used as starting point to run molecular dynamics simulations.

Molecular dynamics trajectories were computed at a constant temperature of 300 K by coupling the system to a thermal bath, using Berendsen's algorithm [33] as implemented in the AMBER suite of programs, with a time constant of 0.2 ps for heat bath coupling. Time step was set to 1 fs, and the list of nearest neighbors was updated every 15 steps and using a distance dependent dielectric constant of 1r. Initial structures were heated in a stepwise manner at a rate of 30 K every 10 ps. When the system achieved 300 K, only 20 ps were required to equilibrate the systems, after which a 1 ns trajectory followed.

Molecular dynamics of the Bcl-2 /X(16BH3) complexes

Although there is a X-ray diffraction 3D structure of Bcl-2, available from the Protein Data Bank (entry 1G5M), due to the large induced fit observed in Bcl-x_L when complexed with Bak(16BH3) (root-mean-square deviation (rmsd) of the backbone atoms observed between the structures of Bcl-x_L (entry 1MAZ) and Bcl-x_L/Bak(16BH3) (entry 1BXL) of 1.1 Å) and the high sequence identity exhibited between Bcl-2 and Bcl-x_L, it was considered more appropriate to construct a starting structure of the Bcl-2/Bak(16BH3) complex by homology modeling using the structure of Bcl-x_L/Bak(16BH3) as template.

Homology modeling was carried out using the previously optimized Bcl-x_L/Bak(16BH3) structure as template by means of the AMBER suite of programs [31]. Side chains of the non-conserved residues were generated in an extended conformation using the EDIT module of AMBER. The structure was optimized in a stepwise manner following the same protocol as with the Bcl-x_L/X(16BH3) complex. Analysis of the minimized Bcl-2/Bak(16BH3) structure with PROCHECK [34] shows that 79.3% of the residues of Bcl-2 lie on the most favored regions of the corresponding Ramachandran maps and furthermore, 19.9% lie on the allowed regions. These figures are similar to those computed for Bcl-2 (entry 1G5M) (78.3% and 19.6%, respectively) and Bcl-x_L (entry 1MAZ) (76.8% and 20.8%, respectively).

The rmsd of Bcl-2 in the complex constructed by homology modeling in the present work and the experimental structure of the isolated protein is 1.9 Å. On the other hand, rmsd of Bcl-2 in the Bcl-2/X(16BH3) complex with the Bcl-x_L experimental structure and with Bcl-x_L in the Bcl-x_L/Bak(16BH3) experimental structure is 2.0 and 1.1 Å, respectively. For the computations of the rmsd the backbone atoms of both structures were considered, although those of the flexible loop located between helix 1 and 2 (residues 34–91), the first eight residues of the N-terminus, the four last residues of the C-terminus, as well as helix 3 (residues 110–125), were excluded from the calculation. As ex-

Table 1a. Average values of angles and distances for Bak (16BH3) – Bcl-x_L.

Bak(16BH3) – Bcl-x_L DISTANCES (Å)	
ARG 76 (*HH21*) – GLU 129 (*OE2*)	1.72 ± 0.14
ASP 83 (*OD2*) – ARG 139 (*HH12*)	1.80 ± 0.18
ASP 83 (*OD1*) – ARG 139 (*HH22*)	1.68 ± 0.01
ASP 84 (*OD2*) – ARG 103 (*HH22*)	1.75 ± 0.13
ASP 84 (*OD2*) – ARG 103 (*HH12*)	1.85 ± 0.19
ASP 84 (*OD1*) – ARG 204 (*HH12*)	1.85 ± 0.26
ASP 84 (*OD1*) – ARG 204 (*HH22*)	1.75 ± 0.14
Bak(16BH3) - Bcl-x_L ANGLES (°)	
ARG 76 (NH2-*HH21*) – GLU 129 (*OE2*)	159.5 ± 10.4
ASP 83 (*OD2*) – ARG 139 (*HH12-NH2*)	160.3 ± 10.6
ASP 83 (*OD1*) – ARG 139 (*HH22-NH2*)	164.9 ± 7.6
ASP 84 (*OD2*) – ARG 103 (*HH22-NH2*)	145.8 ± 12.2
ASP 84 (*OD2*) – ARG 103 (*HH12-NH1*)	153.2 ± 7.9
ASP 84 (*OD1*) – ARG 204 (*HH12-NH1*)	145.8 ± 12.2
ASP 84 (*OD1*) – ARG 204 (*HH22-NH2*)	147.4 ± 10.9

Table 1b. Average values of angles and distances for Bax (16BH3) - Bcl-x_L.

Bax(16BH3) - Bcl-x_L DISTANCES (Å)	
GLU 61 (*OE1*) – ARG 132 (*HH21*)	1.71 ± 0.14
LYS 64 (*HZ2*) – ASP 133 (*OD2*))	1.85 ± 0.43
GLU 69 (*OE1*) – ARG 103 (*HH22*)	1.72 ± 0.11
GLU 69 (*OE1*) – ARG 100 (*HE*)	1.82 ± 0.20
ASP 71 (*OD1*) – TYR 195 (*HH*)	1.46 ± 0.11
ASP 71 (*OD2*) – ARG 139 (*HH12*)	1.80 ± 0.21
ASP 71 (*OD2*) – ARG 139 (*HH22*)	1.80 ± 0.16
Bax(16BH3) - Bcl-x_L ANGLES (°)	
GLU 61 (*OE1*) – ARG 132 (*HH21-NH2*)	145.0 ± 9.8
LYS 64 (*NZ-HZ2*) – ASP 133 (*OD2*)	152.4 ± 32.5
GLU 69 (*OE1*) – ARG 103 (*HH22-NH2*)	164.3 ± 7.4
GLU 69 (*OE1*) – ARG 100 (*HE-NE*)	152.2 ± 10.8
ASP 71 (*OD1*) – TYR 195 (*HH-NH*)	169.5 ± 5.8
ASP 71 (*OD2*) – ARG 139 (*HH12-NH1*)	151.4 ± 9.2
ASP 71 (*OD2*) – ARG 139 (*HH22-NH2*)	151.2 ± 8.5

pected, these results suggest that the structure of Bcl-2 in the Bcl-2/X (16BH3) complex constructed by homology modeling is more similar to the structure of Bcl-x_L in the Bcl-x_L/Bak (16BH3) complex than to the isolated Bcl-2 (1G5M) or Bcl-x_L(1MAZ) structures.

Table 1c. Average values of angles and distances for Bid (16BH3) – Bcl-x_L (DB = dynamic bond).

Bid(16BH3) - Bcl-x_L DISTANCES (Å)	
ARG 88 (*HH21*) – GLU 129 (*OE1*)	DB
ASP 95 (*OD1*) – ARG 139 (*HH12*)	1.71 ± 0.16
ASP 95 (*OD2*) – ARG 139 (*HH22*)	1.74 ± 0.14
ASP 98 (*OD1*) – ARG 204 (*HH12*)	2.47 ± 1.60
ASP 98 (*OD1*) – ARG 204 (*HH22*)	2.52 ± 1.69
ASP 98 (*OD2*) – TYR 195 (*HH*)	1.41 ± 0.09
Bid(16BH3) - Bcl-x_L ANGLES (°)	
ASP 95 (*OD1*) – ARG 139 (*HH12-NH1*)	165.3 ± 7.3
ASP 95 (*OD2*) – ARG 139 (*HH22-NH2*)	163.3 ± 8.7
ASP 98 (*OD1*) – ARG 204 (*HH12-NH1*)	141.9 ± 25.2
ASP 98 (*OD1*) – ARG 204 (*HH22-NH2*)	137.9 ± 23.7
ASP 84 (*OD2*) – TYR 195 (*HH-NH*)	170.3 ± 4.6

Table 1d. Average values of angles and distances for Hrk (16BH3) – Bcl-x_L (DB = dynamic bond).

Hrk(16BH3) – Bcl-x_L DISTANCES (Å)	
LYS 38 (*HZ2*) – ASP 133 (*OD1*)	DB
LYS 38 (*HZ2*) – ASN 136 (*OD1*)	DB
ASP 42 (*OD1*) – ARG 139 (*HH12*)	1.87 ± 0.31
ASP 42 (*OD1*) – ARG 139 (*HH22*)	1.76 ± 0.17
GLU 43 (*OE1*) – ARG 103 (*HH22*)	1.73 ± 0.15
GLU 43 (*OE2*) – ARG 103 (*HH12*)	1.68 ± 0.08
Hr(16BH3) - Bcl-x_L ANGLES (°)	
ASP 42 (*OD1*) – ARG 139 (*HH12-NH1*)	148.9 ± 10.4
ASP 42 (*OD1*) – ARG 139 (*HH22-NH2*)	151.7 ± 10.2
GLU 43 (*OE1*) – ARG 103 (*HH22-NH2*)	161.5 ± 9.3
GLU 43 (*OE2*) – ARG 103 (*HH12-NH1*)	164.2 ± 7.6

Results and discussion

Different geometrical parameters of those residues involved in the interaction between the different apoptosis inhibitor hexadecapeptides and Bcl-x_L or Bcl-2 were monitored along the MD trajectories computed in the present work. For the sake of clarity on the discussion of the present results that follows, residues of Bcl-x_L and Bcl-2 involved in the interaction with the different 16BH3 peptide segments are shown in Figure 2.

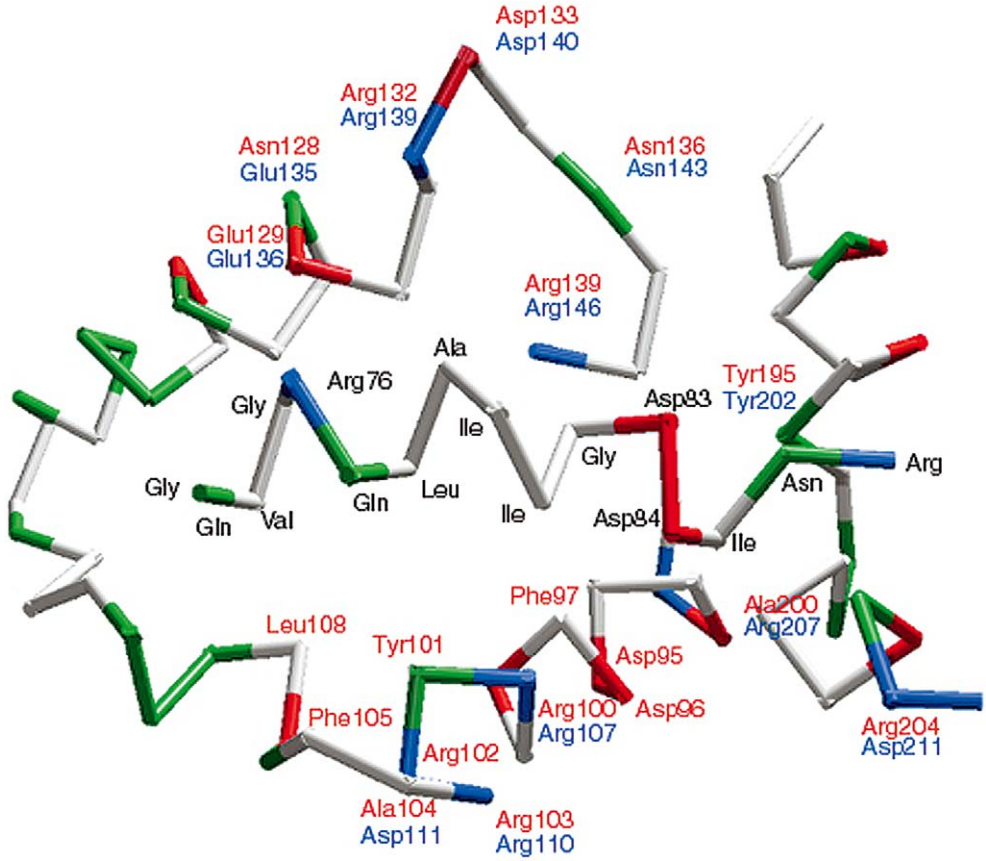

Figure 2. Binding site for Bak peptide on Bcl-x_L (names in red) and Bcl-2 (names in blue). Protein residues are colored according to their type.

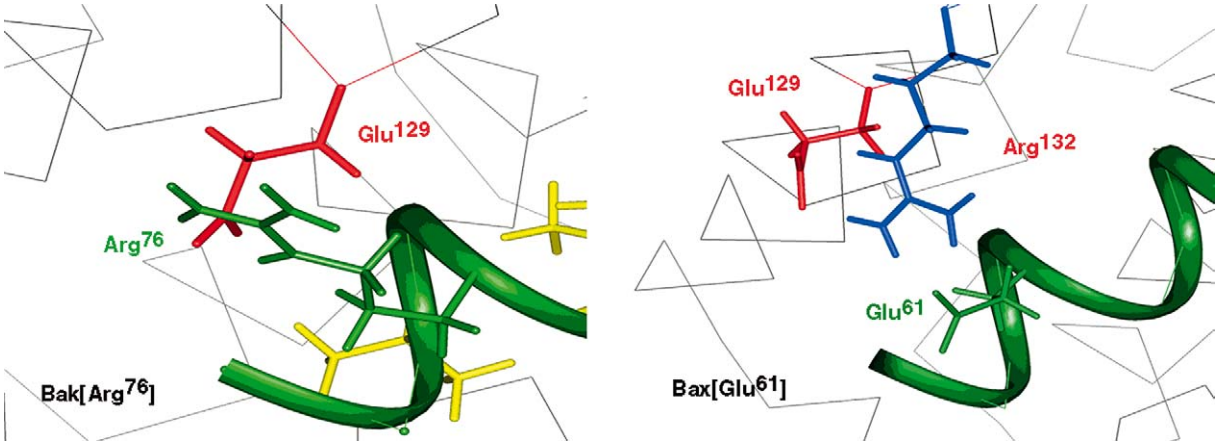

Figure 3. Arrangement of the residues Bak[Arg^{76}] and Bax[Glu^{61}], respectively Glu^{129} of Bcl-x_L.

Bcl-x_L/X(16BH3) complexes

Charged residues identified to play a significant role in the Bcl-x_L/Bak(16BH3) complex along the MD trajectory are listed in Table 1a. Mean values of the structural parameters defining the different interactions during the MD simulation are also included in the table. Residues differ slightly from those proposed by Sattler et al. [30] from the Ala-scan affinity studies of the wild-type sequence. Thus, present results suggest that residues Arg^{76}, Asp^{83} and Asp^{84} play a critical role in the structural stability of the complex. Indeed, the two former are residues also found to be important in the Ala-scan study carried out by Sattler et al. [30]. However, in the same experiments analog [Ala^{84}](72–87)Bak was found to exhibit about the same affinity for Bcl-x_L as the wild-type peptide. This result suggests that affinity of different analogs can be difficult to interpret at the molecular level and it may be that the loss of affinity of this analog is due to the fact that it exhibits a different conformational profile [35].

Table 1b lists different structural parameters of the key residues identified in the structural analysis of the Bcl-x_L/Bax(16BH3) complex during the MD simulation. These residues include Glu^{61}, Lys^{64}, Glu^{69} and Asp^{71}. Sequence alignment identifies Glu^{61} in the same position as Arg^{76} of (72–87)Bak, a residue also found to be important for complex stability. Although, both residues exhibit a different charge, analysis of the respective complexes reveals that both residues interact with different residues of Bcl-x_L. Thus, whereas Arg^{76} interacts with Glu^{129}, Glu^{61} interacts with the nearby residue Arg^{132} via a salt bridge (see Figure 3). Lys^{64} forms a salt bridge with Asp^{133} of Bcl-x_L. This interaction is absent in (72–87)Bak since the corresponding position is occupied by an alanine. However, this result contradicts the yeast two-hybrid experiments of Wang et al. [36] who showed that analog [Ala^{64}, Ala^{65}](57–72)Bax preserves the affinity of the wild type peptide, suggesting that neither Lys^{64} nor Arg^{65} are important for the affinity of the peptide.

Glu^{69} interacts with Arg^{100} of Bcl-x_L. Interestingly, this interaction prevents the previous residue Asp^{68} to interact with Bcl-x_L, in contrast to the role played by its corresponding residue Asp^{83} in (72–87)Bak. This residue is found to be critical for the affinity of the peptide, as deduced from present results as well as from those reported by Sattler et al. [30], who demonstrated that its substitution by alanine induced a loss of affinity for Bcl-x_L. Present results also agree with the studies carried out by Wang et al. [36] reporting that the analog [Ala^{68}](57–72)Bax exhibits the same affinity for Bcl-x_L as the wild type peptide. Similarly, this result is confirmed by the affinity measurements of analog [Ala^{67},Ala^{68}](57–72)Bax [37]. Finally, it is important to stress the importance of the interaction between the residues Asp^{71} and Arg^{139} of Bcl-x_L. This was already pointed out by Wang et al. [36], who observed that substitution of this residue by alanine results in a loss of affinity of (59–75)Bax for Bcl-x_L. This result also explains that the mutation Arg^{139} to Gln^{139} in Bcl-x_L inhibits its antiapoptotic activity of Bax [30].

Table 1c lists the structural parameters of key residues identified in the Bcl-x_L/Bid(16BH3) complex. Interestingly, (84–99)Bid also exhibits an interaction between residue Arg^{88} and residue Glu^{129} of Bcl-x_L, corresponding to positions 76 and 61 of (72–87)Bak and (57–72)Bax, respectively. However, in this case the atoms involved in the interaction are not kept the same during the dynamics simulation; instead the hydrogen of the guanidinium side chain of Arg^{88} interacts alternatively with each of the oxygen atoms of the Glu^{129} side chain. This behavior is usually referred to as a dynamic bond (DB). The analysis of the molecular dynamics trajectory reveals that Asp^{95} is a residue found to be critical for the affinity of Bid to Bcl-x_L, which is aligned with Asp^{68} in Bax. Similarly, Asp^{98} is identified as a key residue for the stability of the complex, playing the same role as Asp^{71} of (57–72)Bax.

Finally, Table 1d lists the structural parameters of the key residues involved in the Bcl-x_L/Hrk(16BH3) interaction. In this case, residues Lys^{38}, Asp^{42} and Glu^{43} are identified as key residues for the stability of the complex. Lys^{38}, similarly as Lys^{64} of Bax(57–72), interacts with Asp^{133} via a salt bridge. Glu^{43} reinforces the charge-charge interaction through an interaction with Arg^{103}, interaction found in (72–87)Bak and (57–72)Bax.

The analysis of the different interactions reveals that all the peptides studied exhibit two negatively charged residues located on the C-terminus that interact with different residues of Bcl-x_L. In addition, peptides also exhibit a charged residue on the fifth or/and on the eighth positions, the former being either negative or positive, but the latter always positive. Residue number five interacts either with residue Glu^{129} or Arg^{132}, depending on its charge, whereas residue eight always interacts with residue Asp^{133} of Bcl-x_L. However, the charged residue in position eight does not appear to be indispensable for good affinity to Bcl-x_L,

Table 2a. Average values of angles and distances for Bak (16BH3) – Bcl-2.

Bak(16BH3) – Bcl-2 DISTANCES (Å)	
ARG 76 (*HH21*) – GLU 136 (*OE1*)	1.75 ± 0.12
ARG 76 (*HH22*) – GLU 135 (*OE2*)	1.70 ± 0.09
ASP 83 (*OD1*) – ARG 146 (*HH12*)	1.70 ± 0.09
ASP 84 (*OD1*) – TRP 214 (*HE*)	1.77 ± 0.11
ASP 84 (*OD2*) – ARG 110 (*HH22*)	1.68 ± 0.08
Bak(16BH3) – Bcl-2 ANGLES (°)	
ARG 76 (*NH2-HH21*) – GLU 136 (*OE1*)	151.7 ± 7.8
ARG 76 (*NH2-HH22*) – GLU 136 (*OE2*)	162.0 ± 9.3
ASP 83 (*OD1*) – ARG 146 (*HH12-NH1*)	162.2 ± 0.8
ASP 84 (*OD1*) – TRP 214 (*HE-NE1*)	164.0 ± 7.8
ASP 84 (*OD2*) – ARG 110 (*HH22-NH2*)	165.5 ± 6.9

Table 2b. Average values of angles and distances for Bax(16BH3) – Bcl-2 (DB = dynamic bond).

Bax(16BH3) – Bcl-2 DISTANCES (Å)	
LYS 64 (*HZ1*) – ASP 140 (*OD2*)	1.72 ± 0.09
ARG 65 (*HH12*) – ASP 111 (*OD1*)	1.72 ± 0.13
ARG 65 (*HH22*) – ASP 111 (*OD2*)	1.69 ± 0.10
ASP 68 (*OD2*) – ASN 143 (*HD22*)	1.71 ± 0.09
ASP 68 (*OD1*) – ARG 146 (*HH22*)	1.74 ± 0.13
ASP 68 (*OD2*) – ARG 146 (*HH12*)	1.69 ± 0.06
GLU 69 (*OE2*) – ARG 110 (*HH12*)	DB
ASP 71 (*OD2*) – TYR 155 (*HH*)	1.43 ± 0.09
ASP 71 (*OD1*) – ARG 207 (*HH12*)	1.67 ± 0.08
Bax(16BH3) – Bcl-2 ANGLES (°)	
LYS 64 (*NZ-HZ1*) – ASP 140 (*OD2*)	161.2 ± 8.9
ARG 65 (*NH1-HH12*) – ASP 111 (*OD1*)	165.1 ± 7.5
ARG 65 (*NH2-HH22*) – ASP 111 (*OD2*)	165.5 ± 7.2
ASP 68 (*OD1*) – ARG 146 (*HH22-NH2*)	164.5 ± 8.0
ASP 68 (*OD2*) – ASN 143 (*HD22-ND2*)	166.4 ± 6.7
ASP 68 (*OD2*) – ARG 146 (*HH12-NH1*)	165.9 ± 7.3
ASP 71 (*OD2*) – TYR 155 (*HH-OH*)	170.3 ± 5.1
ASP 71 (*OD1*) – ARG 207 (*HH12-NH1*)	169.7 ± 8.4

since the substitution R149A in Bad (corresponding to position 76 in Bak) is still an inhibitor of Bcl-x_L [38].

Bcl-2/X(16BH3) complexes

Table 2a lists key charged residues as well as their structural parameters involved in the interaction of (72–87)Bak with Bcl-2. Comparison with Table 1a

Table 2c. Average values of angles and distances for Bid (16BH3) – Bcl-2 (DB = dynamic bond).

Bid(16BH3) – Bcl-2 DISTANCES (Å)	
ARG 88 (*HH21*) – GLU 136 (*OE1*)	DB
ASP 95 (*OD2*) – ARG 146 (*HH12*)	1.75 ± 0.16
ASP 98 (*OD1*) – TYR 202 (*HH*)	1.48 ± 0.19
ASP 98 (*OD2*) – ASN 143 (*HD21*)	1.75 ± 0.10
Bid(16BH3) – Bcl-2 ANGLES (°)	
ASP 95 (*OD2*) – ARG 146 (*HH12-NH1*)	153.9 ± 10.4
ASP 98 (*OD1*) – TYR 202 (*HH-OH*)	168.9 ± 7.9
ASP 98 (*OD2*) – ASN 143 (*HD21-ND2*)	160.2 ± 8.9

Table 2d. Average values of angles and distances for Hrk (16BH3) – Bcl-2 (DB = dynamic bond).

Hrk(16BH3) – Bcl-2 DISTANCES (Å)	
ARG 36 (*HH22*) – ASP 111 (*OD2*)	1.73 ± 0.11
ARG 36 (*HH21*) – ASP 111 (*OD1*)	1.72 ± 0.10
LYS 38 (*HZ2*) – ASP 140 (*OD1*)	DB
LYS 38 (*HZ2*) – ASN 143 (*OD1*)	DB
ASP 42 (*OD1*) – ARG 146 (*HH22*)	1.72 ± 0.13
ASP 42 (*OD2*) – ARG 146 (*HH12*)	1.77 ± 0.18
GLU 43 (*OE2*) – ARG 107 (*HH21*)	1.77 ± 0.12
GLU 43 (*OE1*) – ARG 110 (*HH11*)	1.76 ± 0.22
Hrk(16BH3) – Bcl-2 ANGLES (°)	
ARG 36 (*NH2-HH22*) – ASP 111 (*OD2*)	161.9 ± 8.8
ARG 36 (*NH1-HH21*) – ASP 111 (*OD1*)	163.0 ± 8.1
ASP 42 (*OD1*) – ARG 146 (*HH22-NH2*)	162.1 ± 8.6
ASP 42 (*OD2*) – ARG 146 (*HH12-NH1*)	160.6 ± 10.2
GLU 43 (*OE2*) – ARG 107 (*HH21-NH2*)	149.7 ± 7.3
GLU 43 (*OE1*) – ARG 110 (*HH11-NH1*)	163.1 ± 9.1

evidences that the peptide exhibits the same interactions with the two target proteins.

Key charged residues involved in (57–72)Bax are listed in Table 2b. Comparison of Tables 2b and 1b shows a different pattern of interactions of the peptide with each of the two proteins. Thus, residue Asp^{68} is key only for the interaction with Bcl-2, whereas residue Glu^{61} is key only for the interaction with Bcl-x_L. Analysis of the structures reveals a different accommodation of the bound conformation of the peptide to the two antiapoptotic proteins. This is due to the difference between Ala^{200} in Bcl-x_L and the corresponding Arg^{207} of Bcl-2. Thus, whereas Asp^{71} forms a hydrogen bond with the latter, it cannot form a hy-

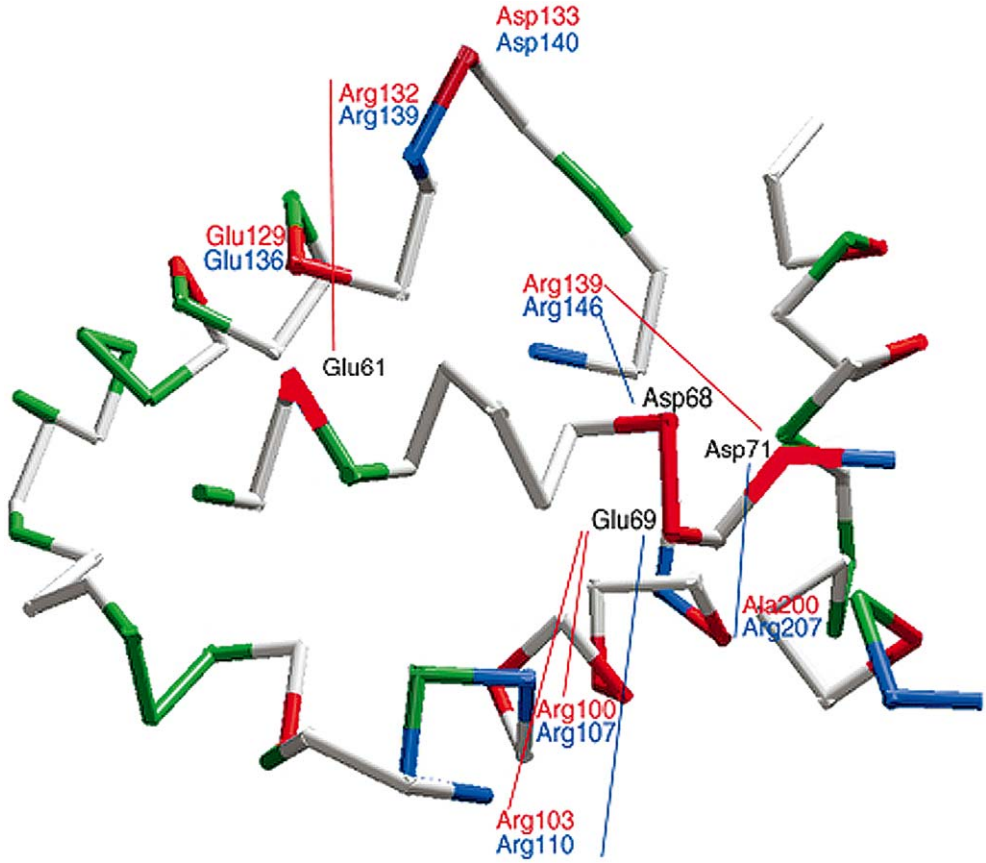

Figure 4. Schematic representation of the interaction of Glu and Asp residues of Bax (16BH3) with Bcl-x_L (red lines) and with Bcl-2 (blue lines). Color of residue names as in Figure 1.

drogen bond with the former. This originates a shift in the pattern of hydrogen bonds between the ligand and the protein, as can be seen in Figure 4. This differential accommodation into the binding groove explains that although the nature of the interaction between Asp^{71} of (57–72)Bax and Bcl-2 is conserved in regard to Bcl-x_L, the residues involved are not the same. On the other hand, the differential interaction of Arg^{65} of (57–72)Bax with Bcl-2 and Bcl-x_L, is due to the different nature of the residues Asp^{111} in Bcl-2 and the corresponding hydrophobic Ala^{104} residue of Bcl-x_L.

Key interactions of (84–99)Bid and Bcl-2 as well as their structural parameters are listed in Table 2c. Interestingly, the interaction between the Arg^{88} and the Glu^{136} is specially important since it is absent in the complex with Bcl-x_L, although analogous to the interaction of Arg^{76} observed in the complexes of (72–87)Bak both with Bcl-x_L and Bcl-2. A second electrostatic interaction occurs between Asp^{95} and Arg^{146} of Bcl-2. This interaction is equivalent to the one with Arg^{139} of Bcl-x_L, and analogous to the interaction between Asp^{83} and Asp^{68} from (72–87)Bak and (57–72)Bax, respectively in their complexes with Bcl-2. Finally, another key residue is Asp^{98} that exhibits its interactions with Tyr^{202} and Asn^{143} of Bcl-2. The same interaction is also present in the Bcl-x_L complex, although in this case residues involved are Tyr^{195} and Arg^{204}, due to the nature of the negatively charged residue aligned with Arg^{204}, being Asp^{211} in Bcl-2.

Key charged residues of (31–46)Hrk, as well as the structural parameters characterizing their interaction with Bcl-2 are listed in Table 2d. MD simulations identify residues Arg^{36}, Lys^{38}, Asp^{42} and Glu^{43}, being the two latter with residues Arg^{146} and Arg^{110} respectively, analogous to all the sequences 16BH3 studied. Additional differences are probably caused by the conformational variations produced by the different charge distribution in these sequences.

In summary, the interaction of the hexadecapeptides with Bcl-2 requires a minimum of two

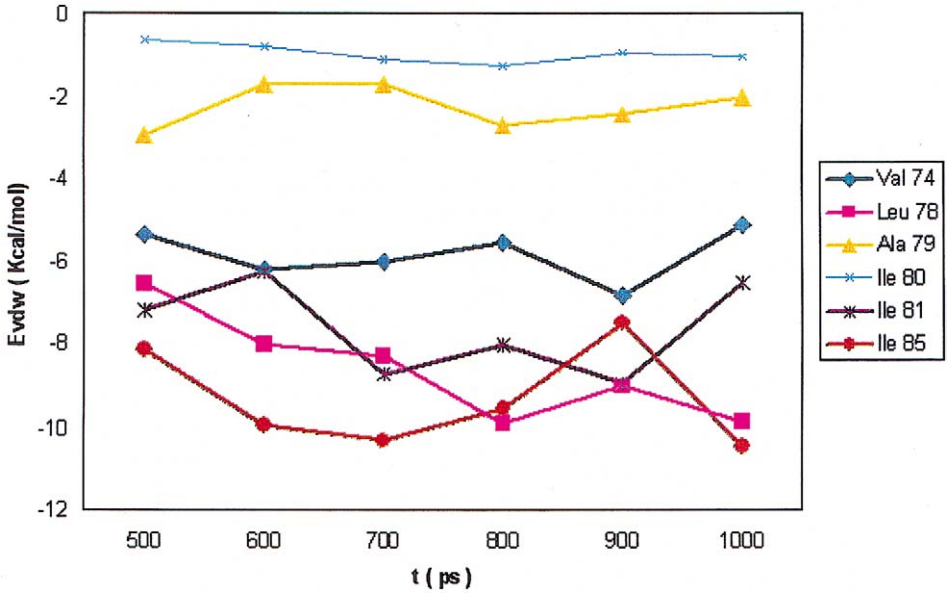

Figure 5. Contribution of hydrophobic residues to the total van der Waals energy along the molecular dynamics trajectory.

charge-charge interactions, either in the positions 12 and 13 or 12 and 15, increasing ligand affinity by addition of charged residues in positions close to these. Moreover, affinity appears to be increased by a positively charged residue in the positions 5, 6 or 8.

From the results discussed above it is possible to establish the minimum requirements for a ligand to exhibit affinity to Bcl-x_L or Bcl-2. The interaction with Bcl-x_L requires the presence of a negative charge in positions 13 and 15. Moreover, the affinity is increased when a positively or negatively charged residue is found in position 5. It appears that a positive charge in position 8 does not contribute significantly to increase their affinity for Bcl-x_L, since Hrk exhibits a charged residue in this position and does not exhibit a significant interaction with the target protein.

On the other hand, the interaction of the hexadecapeptides with Bcl-2 requires the existence of a charged residue in positions 12 and 13. Affinity can be increased by an additional positively charged residue in positions 5 and 8 and a negatively charged residue in position 15. The importance of this latter residue explains the results obtained by Wang et al. [36], who observed that the substitution [Ala^{71}](57–72)Bax decreases its affinity for Bcl-x_L, but not for Bcl-2.

Finally, it is important to stress that the number of intermolecular contacts in a peptide-protein complex is not always enough to explain the observed ligand binding affinity. Other explanations, like propensity of the peptide to form a helix, should also be taken into account [39].

Hydrophobic interactions

The analysis of the hydrophobic interactions of the different peptide fragments with the corresponding proteins was carried out by computing the van der Waals contribution of each residue of the peptide fragment to the peptide-protein interaction energy. The results obtained are similar for all the cases studied in this work. As an example, Figure 5 shows the contributions to the van der Waals term of the interaction between the different hydrophobic residues of (72–87)Bak and Bcl-x_L along the MD trajectory. Analysis of the figure shows that Leu^{78}, Ile^{81}, Ile^{85} are the most important residues involved in hydrophobic interactions.

The importance of Leu^{78}, a residue conserved in all the hexadecapeptides, is stressed by the observation that the [Ala^{78}](72–87)Bak analog is impaired to bind to Bcl-x_L [30] and when delivered into intact cells via fusion to the Antennapedia homeoprotein internalization domain, does not exhibit significant cell killing activity [40]. Moreover, analog [Ala^{151}]Bad (equivalent to [Ala^{78}](72–87)Bak) generates a protein that is unable to bind to Bcl-x_L or Bcl-2 *in vitro* and *in vivo* [38]. The other two hydrophobic residues identified in the analysis of the MD trajectory, Ile^{81} and Ile^{85}, are also demonstrated to be important for the peptide-

protein complex as can be deduced from the results of the alanine scan experiments [30].

Pharmacophore hypothesis

Given the complexity of the interactions discussed above, a simplified hypothesis accounting for all types of interactions between the hexadecapeptides and the antiapoptotic proteins Bcl-2 and Bcl-x_L, is necessary in order to search for small molecule mimics of these molecules. A 3-point pharmacophore based on the C-terminal interactions of the peptides studied can accordingly be proposed. This pharmacophore consist of a hydrogen acceptor, mimicking residues 83 or 84 of Bak and two hydrophobic points mimicking positions 81 and 85 of the peptide. Work to discover new small-molecule inhibitors of Bcl-2 using this hypothesis in Structure-Based Computer screening is in progress [41].

Acknowledgements

We are grateful to CESCA and CEPBA for a generous allocation of computer time, granted to the project 'Molecular Engineering'. The Spanish Ministry of Science and Technology supported this work through grant numbers: SAF2002-04325-C03-03 and SAF2002-04325-C03-01.

References

1. Cohen, J.J., Adv. Immun., 50 (1991) 55.
2. Pan, G., O'Rourke, K., Chinnaiyan, A.M., Gentz, R., Ebner, R., Ni, J. and Dixit, V.M., Science, 276 (1997) 111.
3. Screaton, G.R., Xu, X.-N., Olsen, A.L., Cowper, A.E., Tan, R., McMichael, A.J. and Bell, J.F., Proc. Natl. Acad. Sci. USA, 94 (1997) 4615.
4. Nagata, S., Cell, 88 (1997) 355.
5. Chaudhary, P.M., Eby, M., Jasmin, A., Bookwalter, A., Murray, J. and Hood, L., Immunity, 7 (1997) 821.
6. Screaton, G.R., Mongkolsapaya, J., Xu, X-N., Cowper, A.E., McMichael, A.J. and Bell, J.I., Curr. Biol., 7 (1997) 693.
7. McFarlane, M., Ahmad, M., Srinivasula, S.M., Fernandes-Alnemri, T., Cohen, G.M. and Alnemri, E.S., J. Biol. Chem., 272 (1997) 25417.
8. Reed, J.C., Nat. Rev., 1 (2002) 111.
9. Igney, F.H. and Krammer, P.H., Nat. Rev., 2 (2002) 277.
10. Vaux, D.L., Cory, S. and Adams, T.M., Nature, 355 (1998) 440.
11. Hockenbery, D., Núñez, G., Milliman, C., Schreiber, R.D. and Korsmeyer, S.J., Nature, 348 (1990) 334.
12. Nicholson, D.W. and Thornberry, N.A., Science, 22 (1997) 299.
13. Reed, J.C., J. Cell. Biol., 124 (1994) 1.
14. Strasser A., Huang, D.C.S. and Vaux, D.L., Biochim. Biophys. Acta, 1333 (1997) F151.
15. Chao, D.T. and Korsmeyer, S.J., Annu. Rev. Immunol., 16 (1998) 395.
16. Oltvai, Z.N., Milliman, C.L. and Korsmeyer S.J., Cell, 74 (1993) 609.
17. Reed, J.C., Oncogene, 17 (1998) 3225.
18. Kelekar, A. and Thompson, C.B., Trends Cell. Biol., 8 (1996) 324.
19. Li, P., Nijhawan, D., Budihardjo, I., Srinivasula, S.M., Ahmad, M., Alnemri, E.S. and Wang, X., Cell, 91 (1997) 479.
20. Chinnaiyan, A.M., O'Rourke, K., Lane, B.R. and Dixit, V.M., Science, 275 (1997) 1122.
21. Ottilie, S., Wang, Y., Banks, S., Chang, J., Vigna, N.J., Weeks, S., Armstrong, R.C., Fritz, L.C. and Osterdorf, T., Cell Death Differ., 4 (1997) 526.
22. Zou, H., Henzel, W.J., Liu, X., Lutschg, A. and Wang, X., Cell, 90 (1997) 405.
23. Miayake, H., Tolcher, A. and Gleave, M.E., J. Natl. Cancer Inst., 92 (2000) 34.
24. Baba, M., Iishi, H. and Tatsuta, M., Int. J. Cancer, 85 (2000) 260.
25. Wang, J.-L., Liu, D., Zhang, Z.-J., Shan, S., Han, X., Srinivasula, S.M., Croce, C.M., Alnemri, E.S. and Huang, Z., Proc. Natl. Acad. Sci. USA, 97 (2000) 7124.
26. Degterev, A., Lugovskoy, A., Cardone, M., Mulley, B., Wagner, G., Mitchison, T. and Yuan, J., Nat. Cell Biol., 3 (2001) 173.
27. Kim, K.M., Giedt, C.D., Basañez, G., O'Neill, J.W., Hill, J.J., Han, Y.-H., Tzung, S-P., Zimmerberg, J., Hockenbery, D.M. and Zhang, K.Y., Biochemistry, 40 (2001) 4911.
28. Enyedy, I.J., Ling, Y., Nacro, K., Tomita, Y., Wu, X., Cao, Y., Guo, R., Li, B., Zhu, X., Huang, Y., Long, Y.-Q., Roller, P.P., Yang, D. and Wang, S., J. Med. Chem., 44 (2001) 4313.
29. Lugovskoy, A., Degterev, I., Fahmy, A.F., Zhou, P., Gross, J.D., Yuan, J. and Wagner, G., J. Am. Chem. Soc., 124 (2002) 1234.
30. Sattler, M., Liang, H., Nettesheim, D., Meadows, R.P., Harlan, J.E., Eberstadt, M., Yoon, H.S., Shuker, S.B., Chang, B.S., Thompson, C.B. and Fesik, S.W., Science, 275 (1997) 983.
31. Pearlman, D.A., Case, D.A., Caldwell, J.W., Ross, W.E., Cheatman III, T.E., Fergusson, D.M., Seibel, G.L., Singh, U.C., Weiner, P.K. and Kollman, P.A., AMBER v4.1, University of California, San Francisco, 1995.
32. Cornell, W.D., Cieplak, P., Bayly, C.I., Gould, I.R., Mertz Jr., K.M., Ferguson, D.M., Spellmeyer, D.C., Fox, T., Caldwell, J.W. and Kollman, P.A., J. Am. Chem. Soc., 117 (1995) 5179.
33. Berendsen, H.J.C., Postma, J.P.M., Van Gunsteren, W.F., DiNola, A. and Haak, J.R., J. Chem. Phys., 81 (1984) 3684.
34. Laskowski, R.A., MacArthur, M.W., Moss, D.S. and Thornton, J.M., J. Appl. Crystallogr., 26 (1993) 283.
35. Otzen, D.E. and Fersht, A.R., Protein Eng., 12 (1999) 41.
36. Wang, K., Gross, A., Waksman, G. and Korsmeyer, S.J., Mol. Cell Biol., 18 (1998) 6083.
37. Simonian, P.L., Grillot, D.A.M., Merino, R. and Núñez, G.J., Biol. Chem., 271 (1996) 22764.
38. Zha, J., Harada, H., Osipov, K., Jockel, J., Waksman, G. and Korsmeyer, S.J., J. Biol. Chem., 272 (1997) 24101.
39. Petros, A.M., Nettesheim, D.G., Wang, Y., Olejniczak, E.T., Meadowns, R.P., Mack, J., Swift, K., Matayoshi, E.D., Zhang, H., Thompson, C.B. and Fesik, S.W., Protein Sci., 9 (2000) 2528.
40. Holinger, E.P., Chittenden, T. and Lutz, R.J., J. Biol. Chem., 274 (1999) 13298.
41. Rubio-Martinez, J., Pinto, M., Tomás, M.S. and Pérez, J.J., to be published.